Offset between slit position and reference position in MIDI

Konrad R. W. Tristram (tristram@mpifr-bonn.mpg.de)

December 23, 2008

In a first memorandum, dated May 29, 2008, I investigated the y position of the source in MIDI acquisition images and in photometry data with the prism and in high sense mode. The memorandum described a secular shift as well as a small offset between the beams in y direction. The latter has been corrected and all data since April 2008 has a very good beam overlap in y direction as far as I can judge.

Recently the question arose, how well the beam overlap is in x direction and how well the source is centred in the MIDI slit (usually the 200 μm slit, `SLIT_0.2`). To directly address this issue, Thomas Rivinius obtained an extended acquisition for the bright calibrator HD 18884 using the ATs:

1. After acquiring the target with IRIS, a standard MIDI acquisition image was obtained to check if the star is correctly positioned on the reference pixels within MIDI:
   `MIDI.2008-12-19T02_09_23.000_01.fits`
2. Then the slit (`SLIT_0.2`) was inserted and the acquisition image repeated:
   `MIDI.2008-12-19T02_11_17.000_01.fits`
3. Then also the beamcombiner was inserted and two images were taken, one with `SHUT=AOPEN` and one with `SHUT=BOPEN`:
   `MIDI.2008-12-19T02_12_59.000_01.fits` and `MIDI.2008-12-19T02_14_27.000_01.fits`.

The four images are shown in Figs. 1 to 4. The raw frames (on the left) as well as the result after chopping (on the right) are shown for the two detector windows each. The reference positions as of 2008 Apr 16 are indicated by the light blue crosses. The reference positions are $x_{A1} = 29.0$, $y_{A1} = 31.7$ (in window 1) and $x_{B2} = 28.0$, $y_{B2} = 32.0$ (in window 2) in IDL coordinates (counting starts with 0) in the acquisition images or $\tilde{x}_{A1} = 190.0$, $\tilde{y}_{A1} = 78.7$ and $\tilde{x}_{B2} = 189.0$, $\tilde{y}_{B2} = 164.0$ in detector coordinates (counting starts with 1) on the entire detector.

The setup of MIDI for the different observations (from the FITS headers) as well as the parameters of a 2-dimensional Gaussian distribution fitted to the target PSF are given in Table 1.

Finally, profiles in x-direction of rows 30 to 33 (in acquisition image coordinates), that is at the position of the target, are plotted in Fig. 5. The profiles of the raw images (blue) show the sky and tunnel background. For the slit inserted, these profiles correspond to the transmission profile of the slit. They can be used to determine the slit width and its position. The profiles of the chopped images (green) show the PSF of the target. All profiles were normalised to 1.

In Fig. 1, which corresponds to the standard MIDI acquisition image, the tunnel emission as well as the slightly less bright sky emission in the centre is seen in the raw images (left two windows). The chopped images reveal that the source is well centred. This can also be seen from the first row in Table 1: the centres of the Gaussian fits are in almost perfect agreement to the reference coordinates. The largest offset is $\Delta y_{A1} = 0.1$. The PSF profiles in Fig. 5 are symmetric with respect to the reference position.

In Fig. 2 the slit, or better the slits (there is one slit for each beam) were inserted. This can be seen from the elongated apertures of the slits in the raw images. It turns out that the slits are not centred with respect to the reference pixels for both windows, the crosses at the positions of the reference pixels are not in the middle of the bright sky and tunnel emission horizontally. By consequence, the target PSF is also not centred in the slits. The offset is about $\Delta x = +1$ pixel. This can also be clearly seen from the profile cuts in Fig. 5 where the slits are offset with respect to the reference positions (dashed vertical lines) by 1 pixel. The offset in fact already influences the PSF of the target: it becomes slightly (more) elongated, especially for Beam B (Window 2, see leftmost frame in Fig. 2). The axis ratio for the Gaussian fit decreases to 0.82 for Beam A (Window 1) and to 0.74 for Beam B (Window 2, c.f. second row in Table 1). The centres are shifted slightly in direction of the slit and the PSF profiles appear assymetric in Fig. 5, as one side is suppressed at the edge of the slits. Furthermore, when comparing the values of aperture photometry of the source, I obtain a reduction of the counts rates by about 15 % when the slits are inserted.

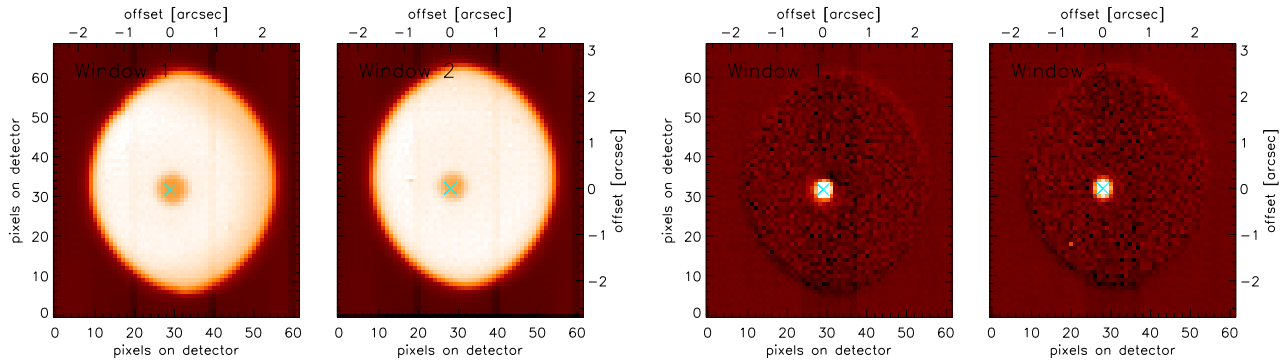

Figure 1: Raw frame (left) and chopped image (right) of `MIDI.2008-12-19T02_09_23.000_01.fits`, i.e. the standard MIDI acquisition image.

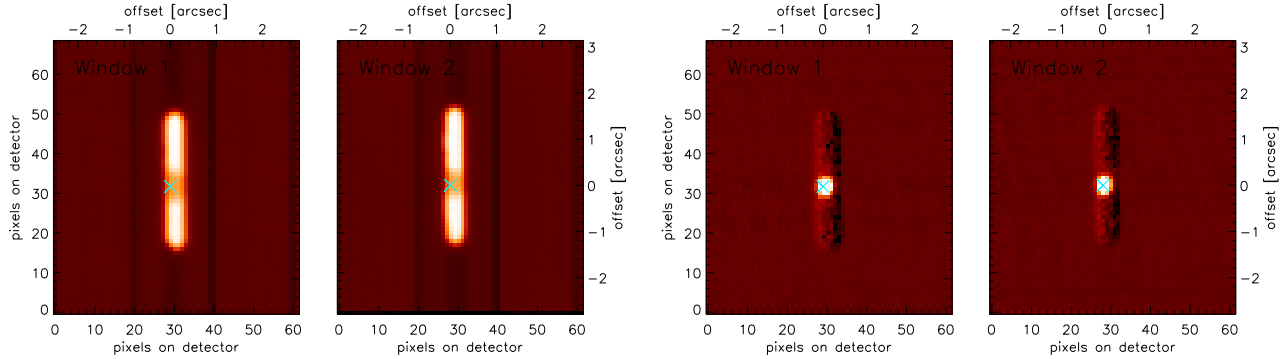

Figure 2: Raw frame (left) and chopped image (right) of `MIDI.2008-12-19T02_11_17.000_01.fits`, i.e. an acquisition image with the slit inserted.

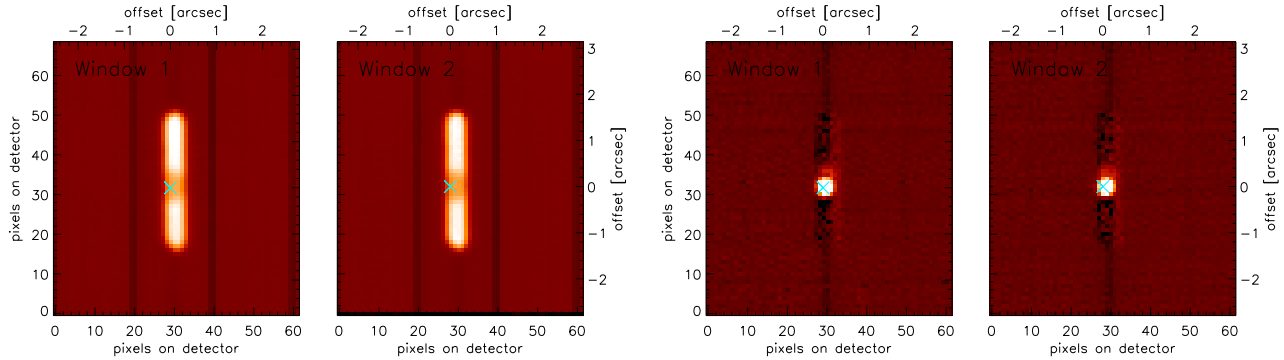

Figure 3: Raw frame (left) and chopped image (right) of `MIDI.2008-12-19T02_12_59.000_01.fits`, i.e. an acquisition image of beam A only with the slit and the beamcombiner inserted.

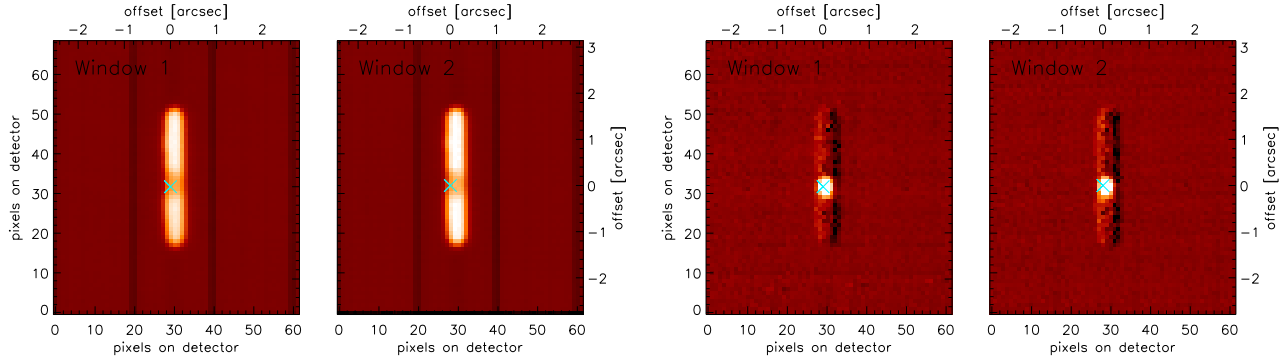

Figure 4: Raw frame (left) and chopped image (right) of `MIDI.2008-12-19T02_14_27.000_01.fits`, i.e. an acquisition image of beam B only with the slit and the beamcombiner inserted.

Image time stamp	MIDI setup			Gaussian fit, WINDOW 1					Gaussian fit, WINDOW 2				
2008-12-19T...	OPTI1	SHUT	SLIT	σ_1	r_1	x_1	y_1	α_1	σ_2	r_2	x_2	y_2	α_2
(1)	(2)	(3)	(4)	(5)	(6)	(7)	(8)	(9)	(10)	(11)	(12)	(13)	(14)
02:09:23	OPEN	ABOPEN	OPEN	1.34	0.93	29.02	31.60	8.14	1.35	0.86	28.01	32.00	2.28
02:11:17	OPEN	ABOPEN	SLIT_0.2	1.28	0.82	29.37	31.72	8.72	1.24	0.74	28.24	32.01	2.41
02:12:59	HIGH_SENS	AOPEN	SLIT_0.2	1.23	0.90	29.40	31.86	10.08	1.20	0.86	28.76	31.89	7.21
02:14:27	HIGH_SENS	BOPEN	SLIT_0.2	1.34	0.72	29.30	31.60	-0.55	1.29	0.70	28.67	31.61	-0.32

Table 1: MIDI configuration for the respective images as well as the parameters of a 2-dimensional Gaussian distribution fitted to the target PSF. The columns are: (1) the time stamp of the FITS file; (2) the beamcombiner setup; (3) the shutter setup; (4) the slit setup; (5) the sigma σ, (6) the axis ratio r, (7) the x-centre, (8) the y-centre and (9) the orientation α of the Gaussian fit for Window 1; (10-14) the same parameters as (5-9) but for Window 2. Accuracies in the target position (x_1, y_1, x_2, y_2) are on the order of 0.2 pixels (corresponding to 80 mas), probably due to residuals in the tip/tilt correction.

Figs. 3 and 4 confirm this conclusion. They essentially only are replications of the Beam A (Window 1) and Beam B (Window 2) frames after the insertion of the beamcombiner. However these images also show that the beam overlap is very good in x direction, the offset being on the order of only 0.1 pixels. In this case the offset is even less than the offset between the beams in y direction, which is about 0.3 pixels (compare the x and y values in rows 3 and 4 of Table 1). That an offset in y direction is present for this observation is actually also seen in a photometry observation (standard MIDI A and B photometry using the prism). The photometry was obtained before the observation sequence described above. Interestingly, the offset between the two beams is sightly wavelength dependent, with the offset increasing towards longer wavelengths (lower x values on the detector, see Fig. 5). Note that the insertion of the beamsplitter leads to a slight change of the target position not only in y but also in x direction, especially for Window 2. The effect is well taken account of by the relative offset in x direction between the two reference positions (at least at the level of accuracy of the current single measurement).

Considering these results, I suggest to adjust the reference pixels once more so that the target PSF lies in the centre of the slit. This is achieved by adding $\Delta x = +1$ pixel to both of the reference pixel positions. The correction should be verified by repeating the experiment described here. I further suggest that the experiment should be repeated once in a while to test for possible drifts in the target position with respect to the MIDI hardware and to verify that the beams still overlap.

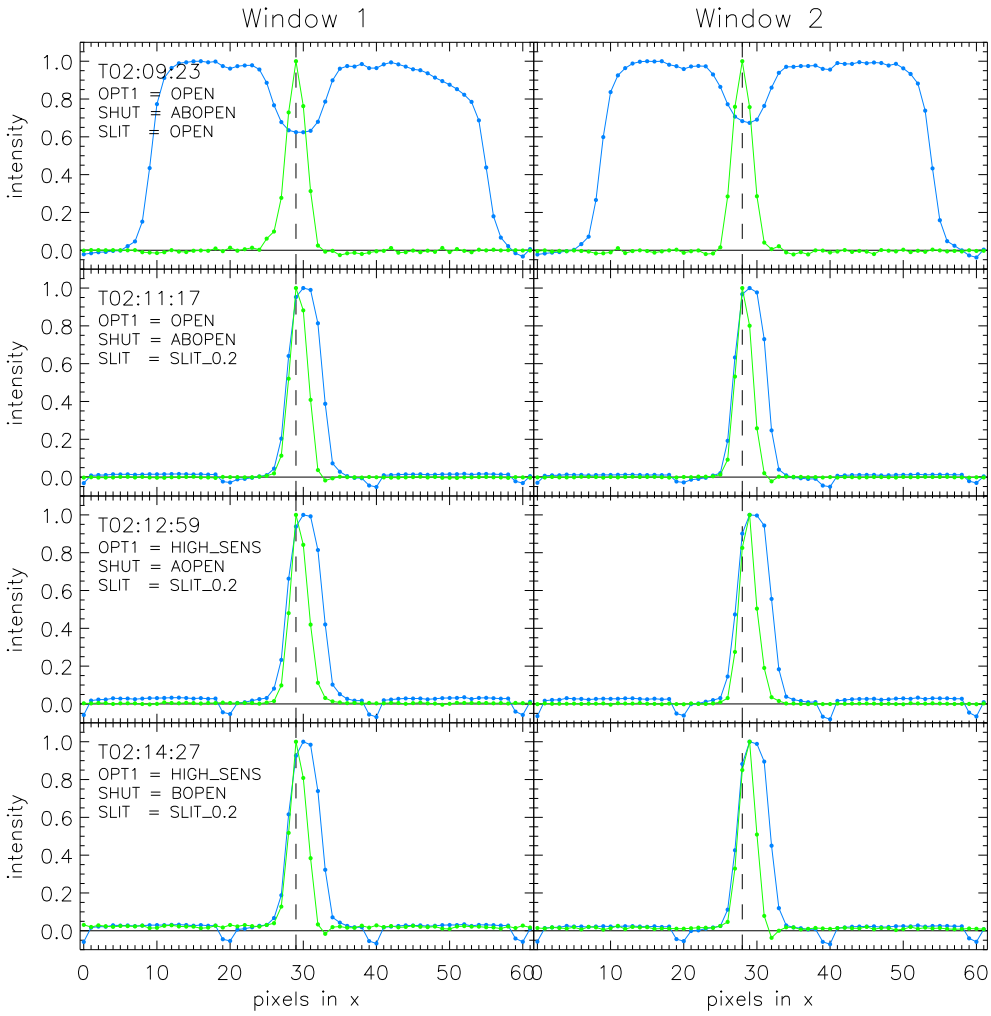

Figure 5: Profiles in x-direction of rows 30 to 33 in the acquisition images for the raw data (blue) and the data after chopping (green). The profiles for Window 1 are plotted in the left column, those for Window 2 in the right column. The dashed vertical lines indicate the x positions of the reference pixels. All profiles were normalised to 1.

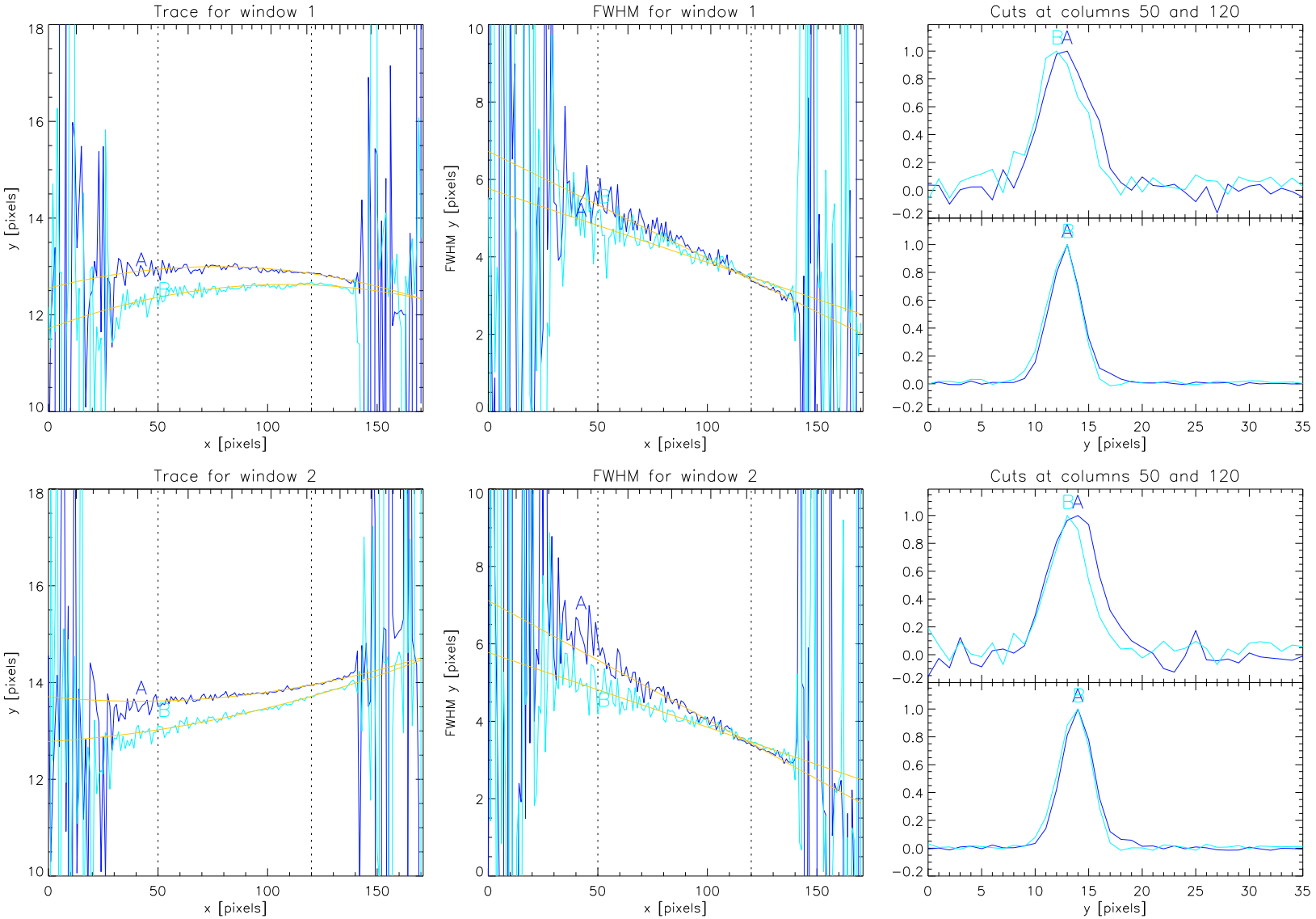

Figure 6: Traces and FWHM for the photometry observed before the extended acquisition sequence discussed in this memorandum. Columns 50 and 120 correspond to 12.5 μm and 8.8 μm respectively. A small, wavelength dependent offset in y direction between the two beams can be seen in the two plots on the left.